

RESEARCH ARTICLE

Photo Degradation of methylene blue in aqueous solution by a new Cu(II)-MOF based on diaminodiphenyl sulfone ligand through response surface methodology (RSM)

Zahra Moseni nik¹, Saeed Jamehbozorgi ^{2*} Majid Ramezani¹, Tahere Momeni Esfahani¹

¹ Department of chemistry, Faculty of sciences, Arak branch, Islamic Azad University, Arak, Iran

² Department of chemistry, Faculty of sciences, Hamedan branch, Islamic Azad University, Hamedan

ARTICLE INFO

Article History:

Received 2019-08-22

Accepted 2020-01-25

Published 2020-05-01

Keywords:

Cu(II)-MOF

Response surface

methodology (RSM)

Degradation pathway

Photocatalyst

Methylene Blue

ABSTRACT

A novel metal-organic framework (MOF), with the formula [Cu(II)L]_n (L= 4, 4'-diamino diphenyl sulfone), has been synthesized conventionally and hydrothermally methods and characterized by FT-IR, PXRD, EDX, and SEM techniques. The results MOFs were applied for photodegradation of Methylene Blue (MB). The influence of affecting variables, such as initial MB dye concentration (2–8mg L⁻¹), Cu(II)-MOF mass (0.01–0.03 mg), pH (3.0–9.0), and time of irradiation (30–90 min). The photocatalytic degradation efficiency was investigated by the central composite design (CCD) methodology. The results of CCD analysis for optimum values of variables revealed that Cu(II)-MOF mass was 0.025g, the initial concentration of MB was 3.51 mg L⁻¹, pH was 4.50 and irradiation time was 75 min. Under the optimum conditions, the photocatalytic MB degradation percentage at the desirability function value of 1.0 was found to be 70%. In addition, the obtained R² value of 0.97 in the regression analysis showed a high photocatalytic efficiency of the proposed method for MB degradation.

How to cite this article

Moseni nik Z., Jamehbozorgi S., Ramezani M., Momeni Esfahani T. Photo Degradation of methylene blue in aqueous solution by a new Cu(II)-MOF based on diaminodiphenyl sulfone ligand through response surface methodology (RSM). J. Nanoanalysis., 2020; 7(2): 141-151. DOI: 10.22034/jna.***.

INTRODUCTION

Dyes usually have an aromatic molecular structure which is resistant to biological degradation. This resistance makes them be stable in the environment, which is important in terms of human health (allergy and skin problems) and the preservation of the environment [1]. In addition, the presence of dyes in the receiving water prevents light penetration due to the creation of eutrophication. This phenomenon leads to disruption of photosynthetic activity and growth of living organisms [1-3]. Among the dyes, used in the different industries, Methylene Blue (MB) (C₁₆H₁₈N₃C₁S) with a molecular weight of 319.85 gmol⁻¹ is more toxic than anionic dyes, and it can easily enter the cells. MB is stored in the Cytoplasm [4-5]. Since MB can cause some diseases such as

nausea, vomiting, mental disorders, and dysuria, removal of MB from sewage is necessary [6].

Due to the low biodegradability of artificial dyes, traditional waste water purification systems, based on biological methods, are not suitable for dyes removal [7]. As a result, commonly used physical and chemical processes such as coagulation and flocculation [8], flotation [9], ultrafiltration membranes [10], electrochemical decomposition [11], ultra-violet radiation [12], sedimentation [13], ozonation [14], use of ultrasound waves recycling, chemical recovery, and adsorption have been used individually or in combination with biological processes to remove dyes efficiently from textile water, and wastewater samples [6-7]. In the meantime, advanced oxidation processes have attracted great attention in recent years due to their ease of use, economic factors, high efficiency, and

* Corresponding Author Email: Email

lack of high amounts of sludge. Advanced oxidation processes are generally referred to processes in which a strong oxidizing agent such as oxygenated water, ozone, and a catalyst such as zinc oxide, iron, and manganese, is used in the presence or absence of an ultraviolet radiation source [15-18].

In recent years, photocatalytic activity of TiO_2 , ZnO or TiO_2/ZnO semiconductors has been investigated to eliminate contaminants in water and wastewater samples [17,19-21]. However, these photocatalysts suffer from the fast recombination of the electron-hole pairs, low solar energy utilization efficiency, and easy agglomeration. Therefore, development of new materials, showing high photocatalytic performance, is of the great importance [19-21].

Metal-organic frameworks (MOFs) are a subclass of coordination polymers with the special features. They are often porous materials, which are constructed from metal centers with bidentate organic ligands. Their inherent large surface areas, uniform but tunable cavities, and tailorable chemistry have enabled them to show a variety of potential applications in drug delivery research and catalytic systems [20-25]. Previous reports on MOF have revealed that the organic linkers in MOF repeating coordination entities can be extended in one, two, or three dimensions. These extended linkers can act as antennas to absorb light and activate the metal clusters via a linker to metal cluster charge transfer in three dimensions, which is similar to the case for inorganic semiconductor quantum dots [26-28]. Indeed, several studies have demonstrated the successful application of MOFs in photocatalytic dye degradation or hydrogen storage. As photocatalysts, MOFs are superior to semiconductors, for their light absorption ability can be more easily tuned by modifications of the metal ions and the organic linkers to achieve efficient utilization of solar energy and promising technology to convert solar energy into chemical energy [29-30]. However, studies on MOF-based photocatalysts are still at their early stages [29-35].

Cu-based MOF materials are extremely attractive since copper is an earth-abundant element and low-cost in order to be used for different purposes. In addition, Cu-containing complexes are commonly used in catalysts and photocatalysts. Moreover, another advantage of

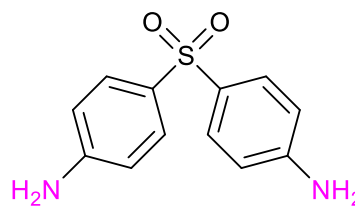


Fig. 1: [L= 4, 4'-diaminodiphenyl sulfone]

using Cu-based MOF materials in photocatalysts is that almost all of the Cu-based MOF materials already reported are visible light responsive due to the existence of extensive copper oxo clusters, which make it possible for a direct excitation of the Cu-O and/or Cu-N clusters under visible light irradiation [36-44]. In this study, the ligand [L= 4, 4'-diaminodiphenyl sulfone] (DDS) which is an antibiotic with many medicinal properties such as treat skin diseases [45], was used to synthesis of MOFs (Fig. 1).

Response surface methodology (RSM) is one of the experimental design methods that is usually used for process modeling [44,46-50]. The possible interactions of different factors on preferred responses can be investigated with RSM by a designed minimum number of experiments. Finally, an optimal condition can be readily obtained.

In the present work, we aimed to report a new Cu(II)-MOF photocatalyst on the basis of DDS in order for photodegradation of MB dye. Firstly, Cu(II)-MOF was synthesized after from conventionally and hydrothermal methods. Furthermore, important parameters, influencing the photocatalytic activity of MB dye such as the pH value, initial dye concentration, and the concentration of photocatalyst, were studied and optimized. Therefore, effects of different factors were investigated, and optimum conditions for degradation of MB were obtained by RSM.

EXPERIMENTAL SECTION

Materials and methods

All experiments were carried out in air and room temperature (25 °C). Starting materials were commercially pure and used without any further purification. Fourier transform infrared (FT-IR) spectra (400-4000 cm^{-1}) were recorded with a BOMEN MB102 FT-IR spectrometer. Powder X-ray diffraction patterns (PXRD) of the Cu(II)-MOFs were obtained with a Philips X-ray diffractometer (Model PW1840) in two areas. In

Table 1. Values and levels of the chosen variables in central composite design.

Factors	Unit	Symbol	Levels				
			- α	Low (-1)	Central (0)	High (+1)	+ α
pH	-	A	3	4.5	6	7.5	9
Mass of MOF	mg	B	0.01	0.015	0.02	0.025	0.03
Initial MB dye concentration	ppm	C	2	3.5	5	6.5	8
Contact time	min	D	30	45	60	75	90

the range of low angle 1-10° using Cu Ka radiation and in usual ranging 20-60° using Cr Karadiation. In addition, the Field Emission Scanning Electron Microscopy (SEM) images were obtained using a Hitachi Japan S4160 scanning electron microscope.

Synthesis of the Cu(II)-MOF

The synthesis of Cu(II)-MOF(1) and Cu(II)-MOF(2) have been done with two methods, conventionally (in the room temperature) and hydrothermally (12h at 200 °C), respectively. In a typical synthesis of Cu(II)-MOF(1), 2 mmol of ligand [L= 4, 4'-diaminodiphenyl sulfone] (DDS) was added to methanol (CH₃OH) (15 mL), and the mixture was stirred at room temperature (25 °C) for 10 min. 1 mmol of CuSO₄ salt was dissolved

in 15 mL methanol (CH₃OH), and then mix the solutions and the resulting mixture was stirred for another 45 min. Then 5 ml of sodium hydroxide (NaOH) solution 0.1 M was added dropwise to the mentioned mixture. After the addition of the NaOH solution, the mixture was further stirred for 2 h at 50 °C. The mixture was then centrifuged and the obtained green color precipitate was washed with methanol (3'5mL) and dried in vacuum (70% yield based on Cu) [51].

The synthesis of Cu(II)-MOF(2) is done by using previously reported hydrothermal method [52]. For the synthesis of Cu(II)-MOF(2) at first, 2 mmol of ligand [L= 4, 4'-diaminodiphenyl sulfone] (DDS) and 1 mmol of CuSO₄ were dissolved in 15 mL of methanol (CH₃OH) in separate vessels. Then the reaction solution and 5 mL of sodium hydroxide (NaOH) solution 0.1 M transferred into a Teflon-lined autoclave and were heated at 200°C K for 12 h. The green sediment was washed with DMF-ethanol mixture and dried.

Photocatalytic Experiments

To measure the photocatalytic activity of Cu(II)-MOF(2), MB solution was prepared with different concentrations of dye, ranging from 2 to 8 mg L⁻¹,

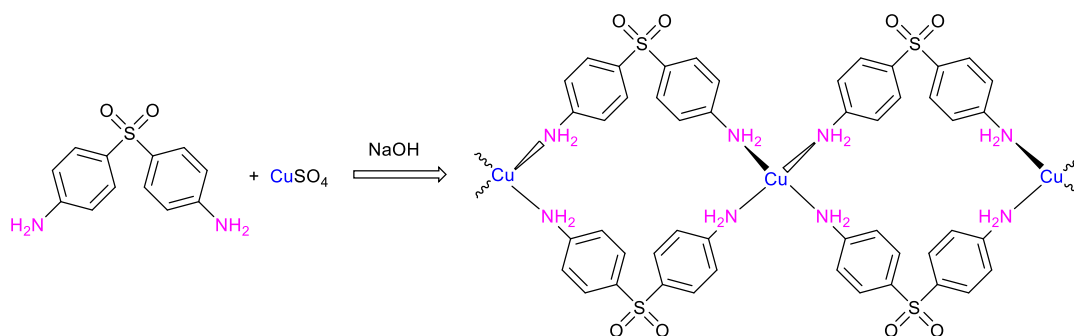
by dissolving the dye powder in pure water. 100 mL of the dye solution was put in the photoreactor and stirred gently in a dark condition for 30 min. The Cu(II)-MOF(2) was added to the dye solution, and the stirring was continued in the dark for another 60 min with the objective to detect any redox processes and check dye absorption by the Cu(II)-MOF(2) which can change the degradation rate. The mixture was centrifuged and the concentration of MB was determined by the UV-Vis spectroscopy. The photoreactor consisted of a magnetic stirrer, thermometer, and two 5W UV lamps. The reactor was put in a dark medium to prevent it from the other ultraviolet sources like the sun's ultraviolet (UV) radiation. In this reactor, a mixture of dye solution and the synthesized MOF was stirred and illuminated with light. The sample measurements were repeated with an interval of 30 min. The MOF was separated from the sample solutions, and the concentration of dye was measured by the same method, used for the dark condition.

Central Composite Design

For studying the photocatalytic activity, the chemometric approach was applied using a central composite design (CCD). Analysis of the experimental data was performed by the Design Expert (version 7) software. The effects of four independent variables (initial MB dye concentration, Cu(II)-MOF(2) mass, pH, and time of irradiation) on the photocatalyst activity of Cu(II)-MOF(2) were presented in Table 1. From the table, it can be seen that the five levels for controlling factors are: pH as the factor A, 3.00, 4.50, 6.00, 7.50, and 9.00; mass of MOF as the factor B, 0.01, 0.015, 0.02, 0.025, and 0.03 mg; initial MB dye concentration as the factor C, 2.00, 3.50, 5.00, 6.50, and 8.00 ppm; and contact time as the factor D 30, 45, 60, 75, and 90 min. Thus, a total of 30 experimental runs were conducted in the present work. The experimental design matrix and the responses are compiled in Table 2.

Table 2. Experimental design matrix and the value of responses based on experiment run.

Run	Factors				Deradation efficiency (%)		
	A	B	C	D	Experimental	Predicted	Residual
1	4.50	0.025	3.50	45.00	42.10	41.06	1.04
2	6.00	0.020	5.00	60.00	20.99	21.59	-0.6
3	6.00	0.020	5.00	60.00	21.24	21.59	-0.35
4	6.00	0.020	8.00	60.00	24.03	24.88	-0.85
5	4.50	0.015	3.50	45.00	29.74	29.01	0.73
6	7.50	0.025	3.50	75.00	24.21	24.17	0.04
7	7.50	0.025	3.50	45.00	10.17	9.86	0.31
8	7.50	0.025	6.50	75.00	9.56	10.68	-1.12
9	6.00	0.020	5.00	60.00	22.58	21.59	0.99
10	7.50	0.015	6.50	75.00	5.41	4.96	0.45
11	6.00	0.020	5.00	60.00	21.46	21.59	-0.13
12	7.50	0.015	6.50	45.00	13.95	15.22	-1.27
13	6.00	0.020	5.00	60.00	22.79	21.59	1.2
14	6.00	0.020	5.00	90.00	25.67	25.79	-0.12
15	7.50	0.025	6.50	45.00	10.95	9.17	1.78
16	3.00	0.020	5.00	60.00	60.73	62.84	-2.11
17	6.00	0.020	5.00	60.00	20.49	21.59	-1.1
18	6.00	0.030	5.00	60.00	28.16	30.18	-2.02
19	7.50	0.015	3.50	45.00	5.07	5.93	-0.86
20	7.50	0.015	3.50	75.00	8.22	8.48	-0.26
21	6.00	0.020	5.00	30.00	6.30	7.28	-0.98
22	4.50	0.015	3.50	75.00	45.72	46.01	-0.29
23	6.00	0.020	2.00	60.00	38.66	38.91	-0.25
24	4.50	0.015	6.50	45.00	29.90	28.45	1.45
25	6.00	0.010	5.00	60.00	13.34	12.42	0.92
26	4.50	0.015	6.50	75.00	31.96	32.66	-0.7
27	4.50	0.025	3.50	75.00	70.70	69.82	0.88
28	4.50	0.025	6.50	75.00	48.85	46.5	2.35
29	4.50	0.025	6.50	45.00	30.40	30.53	-0.13
30	9.00	0.020	5.00	60.00	4.96	3.95	1.01



Scheme 1: The synthesis procedure in the preparation of Cu(II)-MOF.

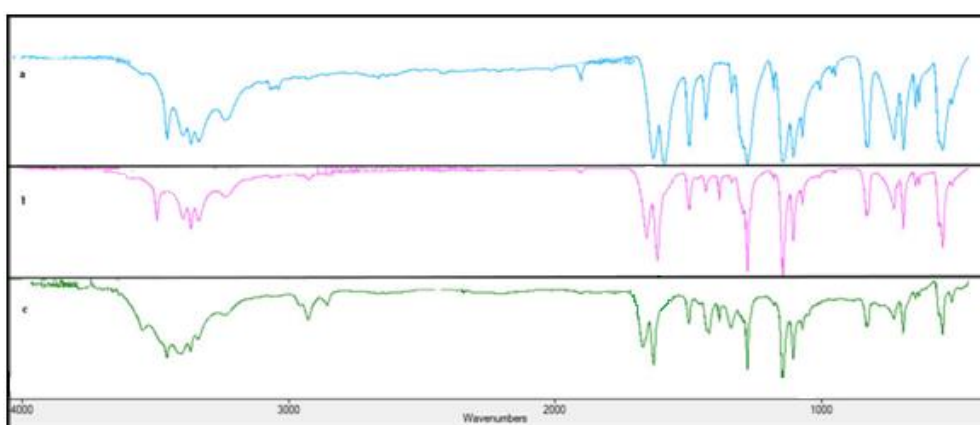


Fig.2. FT-IR spectra of (a) L; (b) Cu(II)-MOF based on $\text{Cu}(\text{NO}_3)_2$; (c) Cu(II)-MOF based on CuSO_4 ;

RESULT AND DISCUSSION

Synthesis and general characterization

The Cu(II)-MOF(1) was prepared in a good yield by a one-pot reaction in a mixture of methanol using ligand [L= 4, 4'-diaminodiphenyl sulfone] (DDS) (Scheme.1). This Cu(II)-MOF(1) is stable in air, moisture, and it is sparingly soluble in polar solvents such as DMF and DMSO. Due to the presence of copper paramagnetic ions in MOF it was not possible to record their NMR spectra. The flexible structure of L has two NH_2 groups in phenyl ring, suitable for coordinate to the Cu(II) ions. In complexes of this ligand, the N-donor atoms adopt ambidentate bridging modes. When copper salt was added to L solution, and the mixture was stirred for 45 min, no precipitate was observed in the mixture of the reaction. But, after addition of the NaOH solution to the reaction, precipitate of Cu(II)-MOF(1) was observed.

In the FT-IR spectrum of MOF 460 cm^{-1} bond was assigned to Cu-N stretching vibration.

Also, in the FT-IR spectrum of the Ligand (DDS), medium bands in the region of 3396 and 3455 cm^{-1} were assigned to the symmetric and asymmetric stretching vibrations of the NH groups. Also, 1590 and 1631 cm^{-1} bond assigned to C=C stretching vibration shifted to 1600 and 1656 cm^{-1} (Fig. 2). These bands slightly shifted to higher wavenumbers (3414 and 3490 cm^{-1}) owing to the bidentate coordination with copper. A strong band, corresponding to the stretching vibration of the S=O bonds of the C-SO₂ groups of the L ligand, appears in the region of 1148 - 1068 cm^{-1} (Fig. 2). [51-53]

Melting points of CuSO_4 and Ligand are 110°C and 183°C while melting point of resulting Cu(II)-MOF is 308°C .

PXRD pattern has been used to examine the phase purity and crystallinity of the Cu(II)-MOFs. The PXRD pattern for ligand and synthesized Cu(II)-MOF (1), Cu(II)-MOF (2) have been represented in Figs. 3 and 4. The characteristic

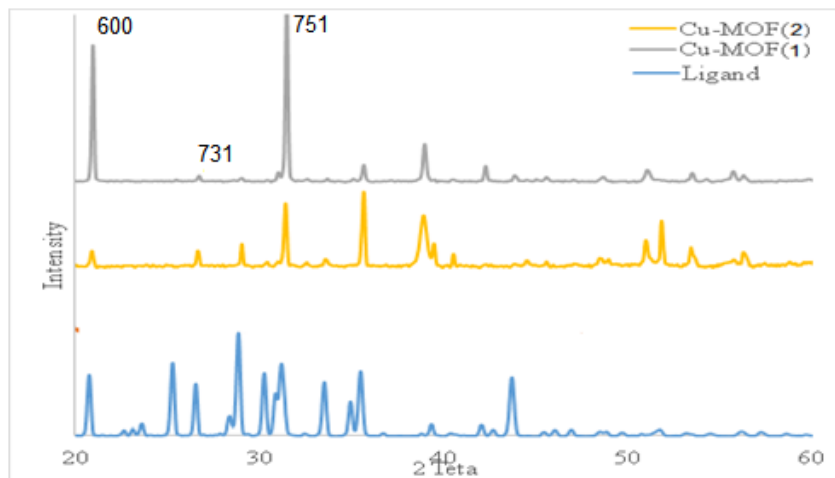


Fig 3. XRD patterns of Ligand, Cu-MOF(1), Cu-MOF(2)

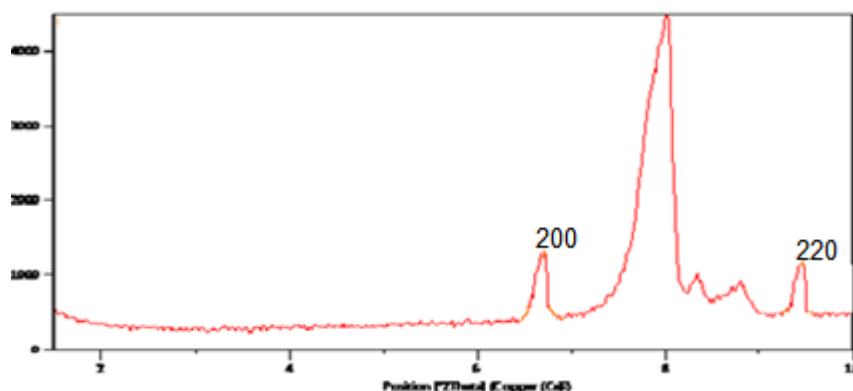


Fig 4. XRD patterns of Cu-MOF(2)

peaks at 2θ values of 5.922° , 6.825° , 9.645° , 20.7913° , 26.5963° , and 31.3706° corresponding to Miller indices (111), (200), (220), (600), (731), and (751), respectively[54-57]Indeed, Cu(II)-MOF(2) displays a better crystallinity ratio than Cu(II)-MOF(1) therefore hydrothermal method was selected for synthesis of MOF and was applied for dye removal.. As pointed out in the FT-IR and XRD patterns of Cu(II)-MOF, based on CuSO_4 , the coordination mode of the L ligand in these MOFs is nearly similar.

The effect of four independent variables, including initial MB dye concentration, Cu(II)-MOF mass, pH, time of irradiation, and their individual, and their interactive impacts on the degradation efficiency (as a response), were investigated in this study using the CCD

method. A quadratic polynomial model was used for development of a mathematical relationship between the responses and the independent variables. The experimental and predicted results for photodegradation efficiency of MB at each point were obtained for different combinations of selected variables (Table 3). The empirical relationship between the photodegradation(%) and different parameters was presented by Eq. (1):

$$\text{Photodegradation \%} = 21.59 - 14.72A + 4.44B - 3.51C + 4.63D - 2.03AB + 2.46AC - 3.61AD - 2.49BC + 2.94BD - 3.2CD + 2.95A^2 - 0.073B^2 + 2.58C^2 - 1.26D^2 \text{Eq. (1)}$$

To evaluate the adequacy of the model, analysis of variance (ANOVA) was used. From the ANOVA of the empirical second-order polynomial model (Table 3), the F-value for the model was obtained to

Table3. ANOVA results for the Response Surface Quadratic Mode.

Source	Sum of square	Degree of freedom	Mean square	F-value	
Model	7745.65	14	553.26	243.73	< 0.0001
A-pH	5202.93	1	5202.93	2292.02	< 0.0001
B-MOF	473.57	1	473.57	208.62	< 0.0001
C-Con.dye	295.47	1	295.47	130.16	< 0.0001
D-Time	514.21	1	514.21	226.52	< 0.0001
AB	65.98	1	65.98	29.06	< 0.0001
AC	96.78	1	96.78	42.63	< 0.0001
AD	209.02	1	209.02	92.08	< 0.0001
BC	99.45	1	99.45	43.81	< 0.0001
BD	138.36	1	138.36	60.95	< 0.0001
CD	163.78	1	163.78	72.15	< 0.0001
A ²	238.85	1	238.85	105.22	< 0.0001
B ²	0.15	1	0.15	0.064	0.8036
C ²	182	1	182	80.18	< 0.0001
D ²	43.83	1	43.83	19.31	0.0005
Residual	34.05	15	2.27	---	---
Lack of Fit	29.92	10	2.99	3.62	0.084
Pure Error	4.13	5	0.83	---	---
Cor Total	7779.7	29	---	---	---

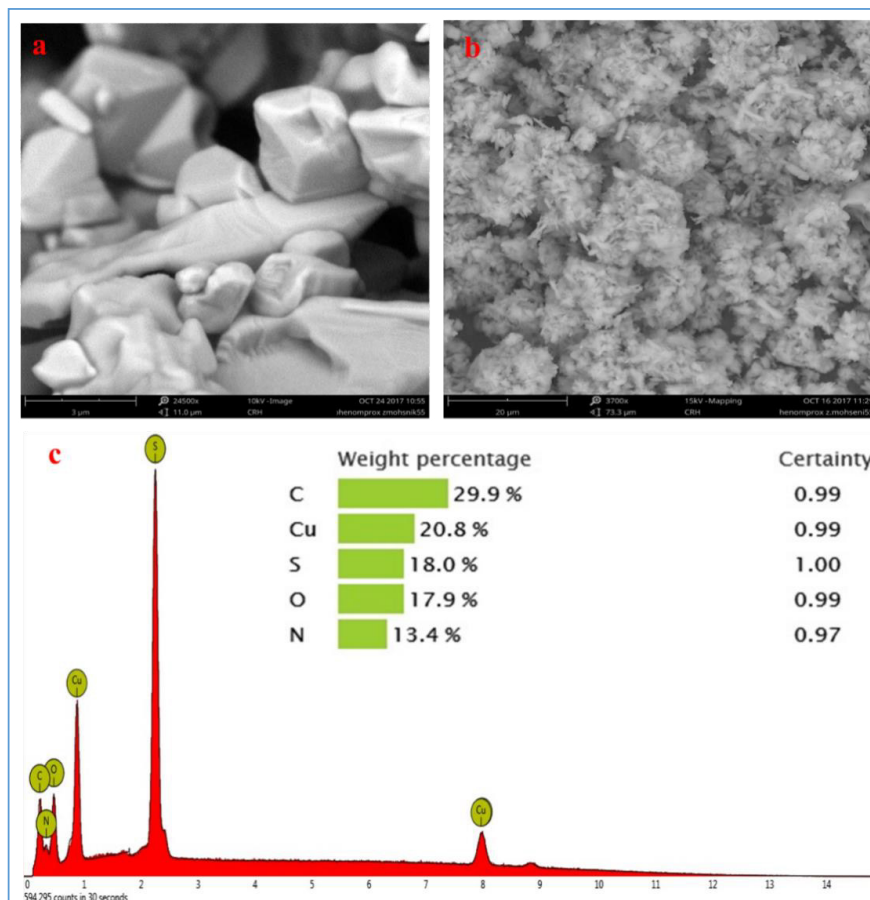


Fig.5. SEM images of Cu(II)-MOF photocatalyst synthesized with variable factors, (a) and (b) Cu-MOF(2) and (c)EDX spectrum of Cu-MOF(1)

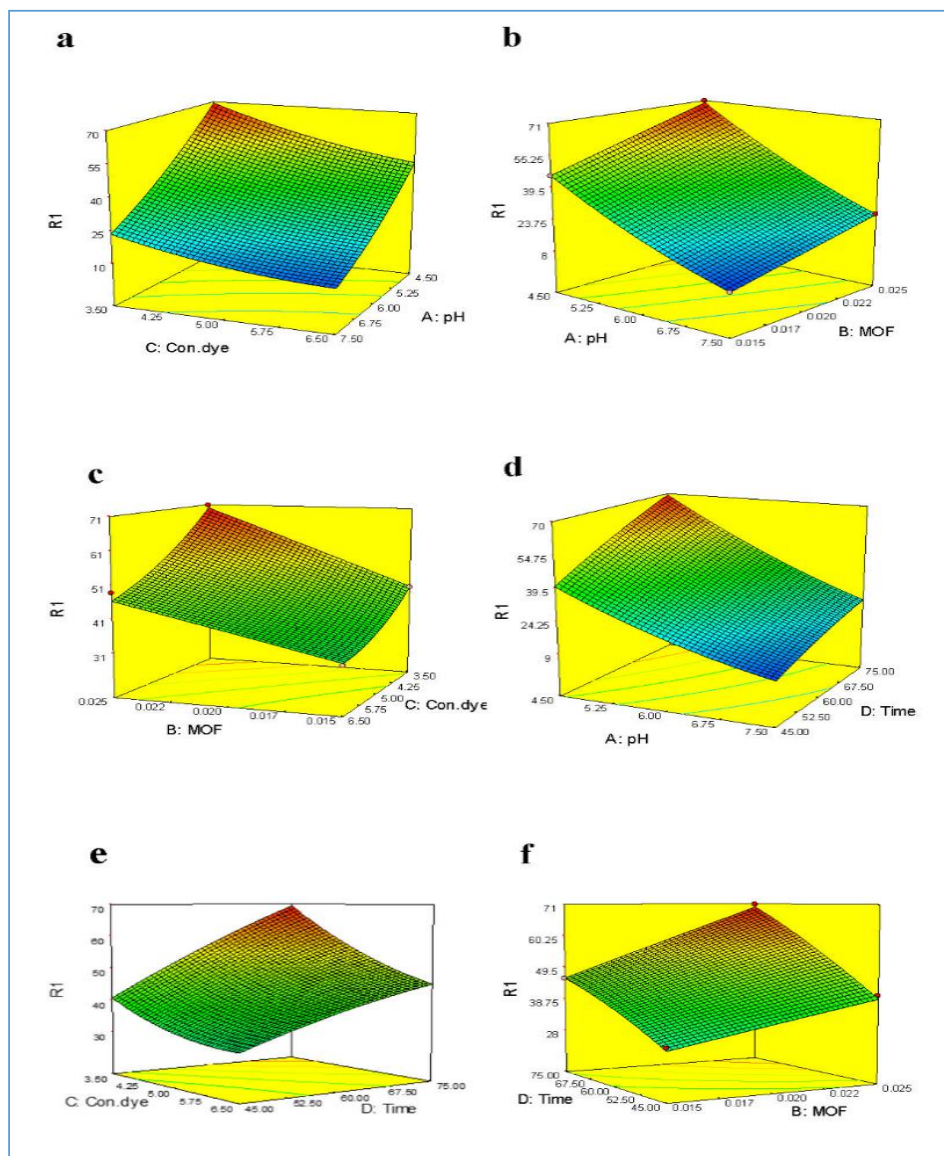


Fig. 6. (a) Effects of pH and initial dye concentration on degradation efficiency of MB, (b) Effects of pH and Cu(II)-MOF mass on degradation efficiency of MB, (c) Effects of Cu(II)-MOF mass and initial dye concentration on degradation efficiency of MB, (d) Effects of pH and contact time on degradation efficiency of MB, (e) Effects of initial MB dye concentration and contact time on degradation efficiency of MB, (f) Effects of contact time and Cu(II)-MOF mass on degradation efficiency of MB.

be243.73, indicating that the model is significant. There is only a 0.01% chance that the “model F-value” could occur due to noise. The model p-value is <0.0001, which also indicates that the model is significant. The “lack-of-fit value” of 3.62 implies that the lack of fit is not significant compared to the pure error. There is a 0.084 chance that the “lack-of-fit F value” could occur due to noise. The “pred R-squared” of 0.9771 is in reasonable agreement

with the “adj R-squared” of 0.9915, confirming good predictability of the model. The results of the interactions between the four independent variables and the responses are shown in Fig. 6. displays that the MB photodegradation efficiency decreases with an increase in the dye concentration and pH value. The reason is that as the concentration of the dye increases, it reduces the penetration of light, absorbing more of the dye onto the surface

Table 4. Comparison of the catalytic efficiency of our CP with that of some reported catalysts.

Catalyst	Dye removal condition	Removal (0/0)	Ref.
[Cu(PDA)(H ₂ O) _{1.5}] _n	200 ml MB, 2ml H ₂ O ₂ ; 100 min	92.5	[61]
[Mn(PDA)(H ₂ O) _{1.5}] _n		85	
[(n-Bu ₃ Sn) ₄ Fe(CN) ₆ ·H ₂ O]	250 ml MB, 20Mm H ₂ O ₂ ;48 h	98	[62]
[(Ph ₃ Sn) ₄ Fe(CN) ₆]	250 ml MB, 30Mm H ₂ O ₂ ;180 min	95	[63]
Fe ₃ O ₄ @SiO ₂	100 ml MB, 4 ml H ₂ O ₂ ;120 min	90-95	[64]
{Cu ₂ (OH) ₂ (bix) ₂ (btc) ₂ (H ₂ O) ₂ }.3H ₂ O} _n		94.0	
[Cu ₂ (bix)(ip) ₂] _n		90.7	
[Cu ₂ (bix)(Meip) ₂] _n	100 ml MB, 0.5 ml H ₂ O ₂ , visible light irradiation; 90 min	89.1	[65]
{Cu ₂ (bix)(pbda) ₂ }.H ₂ O} _n		91.6	
{[Cu ₂ (bix) _{1.5} (pydc) ₂ (H ₂ O)] ₂ .2H ₂ O} _n		82.8	
[Cu ₂ (OH)(mbtx)(sip)(H ₂ O) ₂] _n		76.1	
{[Cu ₂ (OH) ₂ (mbtx)(nip)] ₂ }.H ₂ O} _n	200 ml MB, 1ml H ₂ O ₂ , UV irradiation 180 min	64.9	[66]
[Cu ₂ (OH) ₂ (otrb)(sip)] ₂ .n	200 ml MB, 1ml H ₂ O ₂ , UV irradiation 180 min	91.2	[67]
Fell@ MIL-100(Fe)	50 ml MB	70	[68]
MnO ₂ /Au-NPS nanocomposite	10 ml MB, 60 min	98.9	[69]
Nd ₂ Zr ₂ O ₇ /ZrO ₂	50 ml MB, irradiation with 400w mercury lamp	85	[70]
MOF: [Cu(II)L] _n	100 ml MB, UV irradiation, 75 min	70.70	Present work

of the MOF and occupying active sites on the particle surface and absorbing some uv energy by the dye molecules. These factors reduce the production of radicals and consequently reduce the destruction of pollutants. As Figs. 6b and 5c show the photodegradation of MB rises with an increase in mass of the Cu(II)-MOF and a decrease in the pH value and/or initial concentration of MB. In smaller quantities due to the decrease in the number of particles, the adsorption sites for the dye molecules are reduced, resulting in a decrease in the population of produced radicals and a decrease in removal efficiency. [60] It can be concluded that a decrease in degradation efficiency is observed with an increase in pH value. This effect is more obvious at higher levels of initial dye concentration as can be seen in the contour plots (Fig. 6a). This can be attributed to the surface charge properties of the photocatalyst. The Cu(II)-MOF surface is positively charged in acidic media. As the pH of the solution increases, the number of negatively charged sites goes up.

This reduces the adsorption of dye anions due to electrostatic repulsion. This effect is enhanced with an increase in the dye concentration due to competition for adsorption between the parental dyes and intermediate molecules. As depicted in Figs. 6d-f, the increase in irradiation time (contact time) in third cases shows a significant effect in MB photodegradation.

This behavior can be related to the formation of OH⁻ ions available on the Cu(II)-MOF surface. In

fact, longer irradiation time means more generation of hydroxyl radicals, which are responsible for degradation of the MB dye. A comparison of the absorption power between the MOFs has been made (Table 4)

Optimization was performed on the basis of the desirability function to determine the optimal conditions for the photodegradation of MB. Numerical optimization software was used to identify the specific point that maximizes the desirability function. On the basis of the settings of the software, the optimum conditions for maximum MB photodegradation efficiency (70%) were found to be a pH value of 4.50, an initial dye concentration of 3.51 µg mL⁻¹, an contact time of 75.00 min, and 0.025 mg of Cu(II)-MOF (Fig. 7).

CONCLUSION

In this work, we synthesized and characterized a Cu-based MOF, [Cu(II)L]_n, with a bidentate diaminodiphenyl sulfone derivative ligand after optimization of the synthetic factors for its preparation. The experimental design methodology was applied to optimize different parameters in the photodegradation of MB dye. A quadratic model expressed the functional relationship between the photodegradation efficiency of MB dye and four independent variables including initial MB dye concentration, Cu(II)-MOF mass, pH, and time of irradiation. Under the optimized conditions, the photodegradation efficiency of MB was obtained to be 70%. Also, R² value of 0.9656 in regression

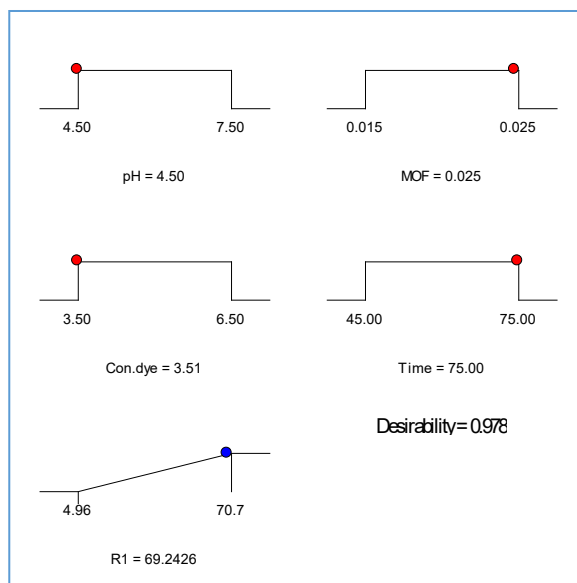


Fig. 7. Optimal conditions for the photodegradation of MB on the basis of the desirability function.

analysis showed a good agreement between the experimental results and the predicted values. Therefore, the Cu(II)-MOF, prepared in this work, can be applied as a suitable candidate for different applications in dye removal.

ACKNOWLEDGEMENT

We thank Islamic Azad University of Arak branch for instruments support.

CONFLICT OF INTEREST

The authors declare that there is no conflict of interests regarding the publication of this manuscript.

REFERENCES

- [1] K.T. Chung, *J. Environ. Sci. Health C*, 34, 233-261 (2016).
- [2] T.M. Fonovich, *Drug Chem. Toxicol.*, 36, 343-352 (2013).
- [3] R. Kabbout and S. Taha, *Biodecol. Phys. Procedia*, 55, 437 (2014).
- [4] A.R. Khataee and M.B. Kasiri, *J. Mol. Catal. A-Chem.*, 328, 8-26 (2010).
- [5] M. Rafatullah, O. Sulaiman, R. Hashim and A. Ahmad, *J. Hazard. Mater.*, 177, 70-80 (2010).
- [6] V.K. Gupta, R. Kumar, A. Nayak, T.A. Saleh and M.A. Barakat, *Adv. Colloid Interface Sci.*, 193, 24-34 (2013).
- [7] M.T. Yagub, T.K. Sen, S. Afroze, & Ang, H.M., *Adv. Colloid Interface Sci.*, 209, 172-184 (2014).
- [8] Y.Y. Lau, Y.S. Wong, T.T. Teng, N. Morad, M. Rafatullah, and S.A. Ong, *RSC Adv.*, 5, 34206-34215 (2015).
- [9] Z. Marczenko, and M. Jarosz, *Analyst.*, 106, 751-756 (1981).
- [10] N. Saffaj, H. Loukili, S.A. Younsi, A. Albizane, M. Bouhria, M. Persinanda, Larbot, *Desalination*, 168, 301-306 (2004).
- [11] M. Panizza, A. Barbucci, R. Ricotti, and G. Cerisola, *Sep. Purif. Technol.*, 54, 382-387 (2007).
- [12] S. Kumar and A.K. Ojha, *J. Alloy Compd.*, 644, 654-662 (2015).
- [13] A.Z. Aroguz, J. Gulen and R.H. Evers, *Bioresour. Technol.*, 99, 1503-1508 (2008).
- [14] J. Zhang, K.H. Lee, L. Cui and T.S. Jeong, *J. Ind. Eng. Chem.*, 15, 185-189 (2009).
- [15] A. Houas, H. Lachheb, M. Ksibi, E. Elaloui, C. Guillard and J.M. Herrmann, *Appl. Catal. B-Environ.*, 31, 145-147 (2001).
- [16] H. Lachheb, E. Puzenat, A. Houas, M. Ksibi, E. Elaloui, C. Guillard and J.M. Herrmann, *Environmental.*, 39, 75-90 (2002).
- [17] N.P. Mohabansi, V.B. Patil and N. Yenkie, *Rasayan j. chem.*, 4, 814-819 (2011).
- [18] W.S. Kuo and P.H. Ho, *Chemosphere.*, 45, 77-83. (2001).
- [19] M.R.D. Khaki, M.S. Shafeeyan, A.A.A. Raman and W.M.A.W. Daud, *J. environ. manage.*, 198, 78-94 (2017).
- [20] J. Li, Y. Ma, Z. Ye, M. Zhou, H. Wang, C. Ma, D. Wang, P. Hou and Y. Yangsheng, *Appl. Catal. B: Environ.*, 204, 224 (2017).
- [21] W. Wan, S. Yu, F. Dong, Q. Zhang and Y. Zhou, *J. Mater. Chem. A.*, 4, 7823-7829 (2016).
- [22] L. Ye, X. Jiao, M. Zhou, S. Zhang, H. Yao, W. Zhao, A. Xia, H. Ade and J. Hou, *Adv. Mater.*, 27, 6046-6054 (2015).
- [23] L. Zhu, X.Q. Liu, H.L. Jiang and L.B. Sun, *Chem. rev.*, 117, 8129-8176 (2017).
- [24] S.K. Elsaidi, M.H. Mohamed, D. Banerjee and P.K. Thallapally, *Coord. Chem. Rev.*, 358, 125-152 (2018).
- [25] Q. Yang, Q. Xu and H.L. Jiang, *Chem. Soc. Rev.*, 46, 4774-4808 (2017).
- [26] F.X. Llabres, I. Xamena, A. Corma and H. Garcia, *J. Phys. Chem. C*, 111, 80-85 (2007).
- [27] C.G. Silva, L. Luz, F.X. Llabres, A. Corma and H. Garcia,

- Chem. A Euro., J., 16, 11133 -11138 (2010).
- [28] M. M. Siddiqui, J.T. Mague and M. S. Balakrishna., *Inorg. chem.*, 54, 6063-6065 (2015).
- [29] K. Nagaveni, G. Sivalingam, M.S.Hegde and G. Madras, *Appl. Cata. B: Environ.*, 38, 1600-1604 (2004).
- [30] W.S. Kuo, P.H. Ho, *Chemosphere.*, 45, 77 -83 (2001).
- [31] D. Wang and Z. Li, *J. Catal.*, 342, 151-157 (2016).
- [32] V. Stavila, A.A. Talin and M.D. Allendorf, *Chem. Soc. Rev.*, 43, 5994-6010 (2014).
- [33] T. Zhang and W. Lin, *Chem. Soc. Rev.*, 43, 5982-5993 (2014).
- [34] Z. Lian, K. Jiang and T. Lou, *RSC Adv.*, 5, 82781-82788 (2015).
- [35] X. He, C. Yang, D. Wang, S.E. Gilliland, D.R. Chena and W.N. Wang, *J. Mater. Chem. A.*, 6, 932-940 (2018).
- [36] X. Shi, J. Zhang, G. Cui, N. Deng, W. Wang, Q. Wang and B. Tang, *Nano Res.*, 11, 979-987 (2018).
- [37] Z.L. Wu, C.H. Wang, B. Zhao, J. Dong, F. Lu, W.H. Wang, W.C. Wang, G.J. Wu, J.Z. Cui and P. Cheng, *Ange. Chem. Inter. Ed.*, 55, 4938 (2016).
- [38] T. Song, L. Zhang, P. Zhang, J. Zeng, T. Wang, A. Ali, H. Zeng., *J. Mater. Chem. A.*, 5, 6013-6018 (2017).
- [39] B. Li, H.M. Wen, Y. Cui, W. Zhou, G. Qian and B. Chen., *Adv. Mater.*, 2, 21-49(2018).
- [40] Y. J.Cheng, R. Wang, Sh. Wang, X. J. Xi, L.Fang Ma, Sh. Zang, *Chem. com.*, 69, (2018).
- [41] J. Zhao, Y. Wang, J. Zhou, P. Qi, S. Li, K. Zhang, X. Feng, B. Wang and C. Hu, *J. Mater. Chem. A.*, 4, 7174-7177 (2016).
- [42] K.L. Haas and K.J. Franz, *Chem. Rev.*, 109, 4921-4960 (2009).
- [43] L.X. Hu, M. Gao, T. Wen, Y. Kang and S. Chen, *Inorg. chem.*, 56, 6507-6511 (2017).
- [44] Y.B. Huang, J. Liang, X.S. Wang and R. Cao, *Chem. Soc. Rev.*, 46, 126-157 (2017).
- [45] S.C. Cho, J.H. Rhim, Y.H. Son, S.J. Lee and S.C., Park, 42, 223-232 (2010).
- [46] A. Witek-Krowiak, K. Chojnacka, D. Podstawczyk, A. Dawiec, K. Pokomeda, *Bioreso. tech.*, 160, 150-160 (2014).
- [47] D.C. Montgomery, "Design and analysis of experiments" John wiley & sons, 2017 Arizona.
- [48] D. Bas, I. H. Boyacı, *J. food eng.*, 78, 836-845 (2007).
- [49] II-H. Cho, K-D. Zoh, *Dye. and Pig. Else. Doi.*, 75, 533-543 (2007).
- [50] M. I.Said, M. Lbrahim, *Mater. Chem. Phys.*, Accepted Manuscript (2019).
- [51] F. NasiriAza, M. Ghaedi,^{K. Dashtian}, S. Hajati V.Pezeshkpour, *Else. Ultrason. Sonochem.*, 31, 383-393 (2016)
- [52] M. I. Said, A. I. El-Said, Aref A.M. Aly, Asia Abou-Taleb, *Ultrason. Sonochem.*, Accepted Manuscript (2018).
- [53] R. Rani, A. Deep, B. Mizaikoff, S. Singh, *Else. Vacuum.*, 164, 449-457 (2019).
- [54] Thi, T. V. N., Luu, C. L., Hoang, T. C., Nguyen, T., Bui, T. H., Nguyen, P. H. D., & Thi, T. P. P, *Adv. Nat. Sci.: Nanosci. Nanotechnol.* 4,035016 (2013).
- [55] N. Al-Janabi, P.Hill, L. Torrent-Murciano, A. Garforth, P. Gorgojo, F. Siperstein, X. Fan, *Else.chem.Eng.*, 281, 669-667 (2015).
- [56] IB. Sun, S. Kayal, A. Chakraborty, *J. Energy.*, 76, 419-427 (2014).
- [57] S.C. Cho, J.H. Rhim, Y.H. Son, S.J. Lee and S.C., Park, *EMM.*, 42, 223-232 (2010).
- [58] L. Chen, J. He, Q. Yuan, Y.W. Zhang, F. Wang, C.T. Au, and S.F. Yin, *RSC Adv.*, 5, 33747-33754 (2015).
- [59] D. Wojcieszak, D. Kaczmarek, J. Domaradzki and M. Mazur, *Inter. J. Materials Science.*, 35, 725-732 (2017).
- [60] A. Teimouria , N. Ghaseda , Sh, Ghanavati Nasabb , S. Habibollahi, *Desalination and Water Treatment.*, 139, 327-341(2018)
- [61] M.I. Said, A.I. El-Said, A.A.M. Aly, A. Abou-Taleb, *Ultrason. Sonochem.*, 46, 68-78 (2018).
- [62] S.E.H. Etaiw, D.I. Saleh, *Acta, Part A.*, 117, 54-60 (2014).
- [63] A.M.A. Ibrahim, S.M.A. Al-Ashqar, *Spectrochim. Acta, Part A*, 92, 238-244 (2012).
- [64] L.-P. Zhang, Z. Liu, Y. Faraj, Y. Zhao, R. Zhuang, R. Xie, X.-J. Ju, W. Wang, L.-Y. Chu, *J. Membr. Sci.*, 573, 493-503 (2019).
- [65] L.-L. Shi, T.-R. Zheng, M. Li, L.-L. Qian, B.-L. Li, H.-Y. Li, *RSC Adv.*, 7, 23432-23443 (2017).
- [66] S. Zhao, T.-R. Zheng, L.-L. Shi, K. Li, B.-L. Li, H.-Y. Li, *J. Mol. Struct.*, 1143, 146-152 (2017).
- [67] S. Zhao, Y.-Q. Zhang, T.-R. Zheng, L.-L. Shi, B.-L. Li, Y. Zhang, *Inorg. Chem. Commun.*, 73, 134-137 (2016).
- [68] H. Lv, H. Zhao, T. Cao, L. Qian, Y. Wang, G. Zhao, *J. Mol. Catal. A: Chem.*, 400, 81-89 (2015).
- [69] X. Bao, Z. Qin, T. Zhou, J. Deng, *J. Environ. Sci.*, 65, 236-245 (2018).
- [70] S. Zinatloo-Ajabshir, Z. Zinatloo-Ajabshir, M. Salavati-Niasari, S. Bagheri, S.B.A. Hamid, *J. Energ. Chem.*, 26,315-323 (2017).